An Essentially Non-Oscillatory (ENO) High-Order Accurate Adaptive Table Model for Device Modeling

Baolin Yang
Cadence Design Systems, Inc.

Bruce McGaughy
Cadence Design Systems, Inc.

ABSTRACT

Modern analytical device models become more and more complicated and expensive to evaluate in circuit simulation. Interpolation based table look-up device models become increasingly important for fast circuit simulation. Traditional table model trades accuracy for speed and is only used in fast-Spice simulators but not good enough for prime-time Spice simulators such as SPECTRE. We propose a novel table model technology that uses high-order essentially non-oscillatory (ENO) polynomial interpolation in multi-dimensions to guarantee smoothness in multi-dimensions and high accuracy in approximating $i-v/q-v$ curves. An efficient transfinite blending technique for the reconstruction of multi-dimensional tables is used. Interpolation stencil is adaptively determined by automatic accuracy control. The method has been proved to be superior to traditional ones and successfully applied in Spectre and Ultrasim for simulating digital, analog, RF, and mixed-signal circuits.

1. INTRODUCTION

The modern device models such as bsim3 and bsim4 become more and more complicated and expensive to evaluate in circuit simulation. An interpolation based table modeling method needs to be continuous at least and C^1 smooth if possible at interpolation boundaries. In table model evaluation, capacitance and conductance are evaluated by taking derivative of the interpolating $i-v/q-v$ polynomials, which makes the $g-v/c-v$ evaluation inherently consistent with the $i-v/q-v$ curves and beneficial for simulation convergence. Traditional table-model methods are either not accurate enough for simulations requiring high accuracy or not robust enough for a wide range of applications.

Because of the accuracy, robustness, and memory consumption concerns, table model technology has not been used in any prime-time Spice simulator such as SPECTRE. We evaluated several table model technology from various sources. One table model method from Bell-Lab uses spline interpolation. Spline interpolation can achieve variation diminishing property by averaging neighboring grid points [1]. This results in a shift of interpolating point away from the original function evaluation point, which has the drawback of smearing the sharp transitions in the $i-v/q-v$ curves such as the sub-threshold region in Mosfets. It has drawbacks of wider stencils, inefficiency in model evaluation, and difficulty in doing local table refinement. ENO interpolation removes the fixed-stencil limitation by using a dynamic stencil to avoid oscillation and keeps the curves' sharpness.

In [2], multi-dimensional interpolation techniques were proposed. Different basis functions along with averaging heuristics were used to achieve smoothness and accuracy of device curves. However, non-polynomial basis function is expensive to evaluate. Averaging technique loses accuracy and is difficult to extend to higher order compared with our systematic approach.

Our locally refined ENO table model solely uses efficient polynomial interpolation. Its dynamic stencil achieves smoothness without making the interpolating stencil wilder, i.e. using more points in interpolation. It is a very flexible and robust method that allows the order to vary according to accuracy requirement, which is due to the fact that unlike existing technologies, the ENO dynamic stencil selection algorithm is systematic and does not depend on order. Indeed, we successfully applied 3rd-order and 4th-order ENO interpolation for diode or mos-diode evaluation. Without high-order interpolation and local refinement technique, it is impossible to have a good approximation of the exponential curve.

Traditional methods only consider the smoothness in one dimension. We found that even if the interpolation is monotone along 1-d table grid lines, the tensor product of these polynomials in multi-dimensions can still give oscillation. We have considered multi-dimensional smoothness by taking advantage of ENO table model's flexibility.

2. ENO INTERPOLATION

Traditional interpolation methods including spline methods are based on fixed stencil interpolations or their averages. For example, to obtain an interpolation for cell i to third order accuracy, the information of the three cells i-1, i and i+1 can be used to build a second order interpolation polynomial. This works well for globally smooth problems. However, fixed stencil interpolation of second or higher order accuracy is necessarily oscillatory near a C^0 corner point. Such oscillations may cause Newton iteration to fail in solving nonlinear circuit equations besides being inaccurate.

Essentially Non-Oscillatory schemes started with the classical paper of Harten et al. in 1987 [4] and have been applied very successfully in computational fluid mechanics. The ENO idea proposed in [4] obtains a self similar (i.e. no mesh size dependent parameter), uniformly high order accurate, yet essentially non-oscillatory interpolation (i.e. the magnitude of the oscillations decays as $O(\Delta v^k)$ where k is the order of accuracy) for piecewise smooth functions. In [4] Harten et al. investigated different ways of measuring local

Permission to make digital or hard copies of all or part of this work for personal or classroom use is granted without fee provided that copies are not made or distributed for profit or commercial advantage and that copies bear this notice and the full citation on the first page. To copy otherwise, to republish, to post on servers or to redistribute to lists, requires prior specific permission and/or a fee.
DAC 2004, June 7–11, 2004, San Diego, California, USA.
Copyright 2004 ACM 1-58113-828-8/04/0006 ...$5.00.

smoothness to determine the local stencil, and developed a hierarchy that begins with one or two cells, then adds one cell at a time to the stencil from the two candidates on the left and right, based on the size of the two relevant Newton divided differences. Although there are other reasonable strategies to choose the stencil based on local smoothness, experience in numerical simulation of nonlinear hyperbolic partial differential equations seems to show that the hierarchy is the most robust for a wide range of grid sizes. We adopt this approach.

ENO interpolation can achieve the property of total variation diminishing up to numerical interpolation error. When we refine the interpolation stencil, ENO method is going to achieve better smoothness. The property of being able to achieve accuracy and smoothness at the same time is very important for its successful application in practical circuit simulation. ENO interpolation calculates local divided difference which reflects oscillation in waveforms and chooses one of the divided difference. For example, second-order interpolation needs a stencil of three points. To find the interpolating polynomial in interval $[v_k, v_{k+1}]$, we may choose either one of stencil $[v_{k-1}, v_k, v_{k+1}]$ and $[v_k, v_{k+1}, v_{k+2}]$ based on the smaller second-order divided difference. For third-order and higher-order interpolation, we have even more flexibility. Dynamic stencil makes interpolation much more smooth and accurate. There are also ways to guarantee the monotonicity of $i-v/q-v$ curves using modified ENO interpolation. However, in our practice, the ENO interpolation turns out to be robust enough. Whenever we observe oscillation in ENO interpolation, it always turns out to be due to the fact that the underlying analytical model has oscillations there.

Given a grid

$$a = v_{\frac{1}{2}} < v_{\frac{3}{2}} < \cdots < v_{N-\frac{1}{2}} < v_{N+\frac{1}{2}} = b, \tag{1}$$

we define cells, cell centers, and cell sizes by

$$I_i \equiv [v_{i-\frac{1}{2}}, v_{i+\frac{1}{2}}],\ v_i \equiv \frac{1}{2}(v_{i-\frac{1}{2}} + v_{i+\frac{1}{2}}),\ \Delta v_i \equiv v_{i+\frac{1}{2}} - v_{i-\frac{1}{2}},\quad i = 1, 2, \cdots, N. \tag{2}$$

We denote the maximum cell size by $\Delta v \equiv max_{1\le i\le N}\Delta v_i$. The first approximation problem we will face is given the cell average of $q(v)$ find a polynomial $p_i(v)$, of degree at most $k-1$, for each cell I_i, such that it is a k-th order accurate approximation to the function $q(v)$ inside I_i. In particular, this gives approximations to the function $q(v)$ at the cell boundaries

In device modeling, the $i-v$ and $q-v$ curves are piecewise smooth and continuous. For such smooth functions, the order of accuracy is defined as whatever accuracy determined by the local truncation error in the smooth regions of the function.

If the function $q(v)$ is only C^0, a fixed stencil approximation may not be adequate near C^0 corner points. Piecewise quadratic interpolation with a fixed one-sided stencil for the step function shows obvious undershoots for the cells near the bottom corner point.

The basic idea in ENO approximation is "adaptive stencil",

$$v_{i-r-\frac{1}{2}}, \cdots, v_{i+s+\frac{1}{2}}\ , \tag{3}$$

namely, the left shift r changes with the location v_i. To achieve this effect, we need to look at the Newton formulation of the interpolation polynomial.

We first review the definition of the Newton divided differences. The 0-th degree divided differences of the function $Q(v)$ are defined by $Q[v_{i-\frac{1}{2}}] \equiv Q(v_{i-\frac{1}{2}})$; and in general the j-th degree divided differences, for $j \ge 1$, are defined inductively by

$$Q[v_{i-\frac{1}{2}}], \cdots, v_{i+j-\frac{1}{2}}] \equiv \frac{Q[v_{i+\frac{1}{2}}, \cdots, v_{i+j-\frac{1}{2}}] - Q[v_{i-\frac{1}{2}}, \cdots, v_{i+j-\frac{3}{2}}]}{v_{i+j-\frac{1}{2}} - v_{i-\frac{1}{2}}}. \tag{4}$$

Similarly, the divided differences of the cell average $\overline{v}$ are defined by

$$\overline{q}[v_i] \equiv \overline{q}_i; \tag{5}$$

and in general

$$\overline{q}[v_i, \cdots, v_{i+j}] \equiv \frac{\overline{q}[v_{i+1}, \cdots, v_{i+j}] - \overline{q}[v_i, \cdots, v_{i+j-1}]}{v_{i+j-\frac{1}{2}} - v_{i-\frac{1}{2}}}. \tag{6}$$

We note that by some derivation,

$$Q[v_{i-\frac{1}{2}}, v_{i+\frac{1}{2}}] = \frac{Q(v_{i+\frac{1}{2}}) - Q(v_{i-\frac{1}{2}})}{v_{i+\frac{1}{2}} - v_{i-\frac{1}{2}}} = \overline{q}_i, \tag{7}$$

i.e. the 0-th degree divided difference of $\overline{q}$ is the first degree divided difference of $Q(v)$. We can thus write the divided differences of $Q(v)$ of first degree by those of $\overline{q}$ of 0-th degree and higher.

The Newton form of the k-th degree interpolation polynomial $P(v)$, which interpolates $Q(v)$ at the $k+1$ points (3), can be expressed using the divided differences (7) by

$$P(v) = \sum_{j=0}^{k} Q[v_{i-r-\frac{1}{2}}, \cdots, v_{i-r+j-\frac{1}{2}}] \prod_{m=0}^{j-1} (v - v_{i-r+m-\frac{1}{2}}). \tag{8}$$

We can take the derivative of (8) to get $p(v)$. We can also express $p(v)$ completely by the divided differences of $\overline{q}$, without any need to reference $Q(v)$.

An important property of divided differences is:

$$Q[v_{i-\frac{1}{2}}, \cdots, v_{i+j-\frac{1}{2}}] = \frac{V^{(j)}(\xi)}{j!}, \tag{9}$$

for $v_{i-\frac{1}{2}} < \xi < v_{i+j-\frac{1}{2}}$, as long as the function $Q(v)$ is smooth in this stencil. Thus the divided difference is a measurement of the smoothness.

We now describe the ENO idea by using (8). Suppose we want to find a stencil of k+1 consecutive points, which must include $v_{i-\frac{1}{2}}$ and $v_{i+\frac{1}{2}}$, such that $Q(v)$ is "the smoothest" in this stencil comparing with other possible stencils. We perform this job by breaking it into steps, in each step we only add one point to the stencil. We thus start with the two point stencil

$$\overline{S}_2(i) = v_{i-\frac{1}{2}}, v_{i+\frac{1}{2}}, \tag{10}$$

where we have used $\overline{S}$ to denote a stencil for the primitive function Q. Notice that the stencil $\overline{S}$ for Q has a corresponding stencil S for $\overline{q}$ through (7), for example (10) corresponds to a single cell stencil $S(i) = I_i$ for $\overline{q}$. The linear interpolation on the stencil $\overline{S}_2(i)$ in (10) can be written in the Newton form as $P^1(v) = Q[v_{i-\frac{1}{2}}] + Q[v_{i-\frac{1}{2}}, v_{i+\frac{1}{2}}](v - v_{i-\frac{1}{2}})$. At the next step, we have only two choices to expand the stencil: we can either add the left neighbor $v_{i-\frac{3}{2}}$, resulting in the following quadratic interpolation

$$R(v) = P^1(v) + Q[v_{i-\frac{3}{2}}](v - v_{i-\frac{1}{2}})(v - v_{i+\frac{1}{2}}). \tag{11}$$

or add the right neighbor $v_{i+\frac{3}{2}}$ which leads to a different interpolation. We note that the derivation from $P^1(v)$ in the interpolation are the same function $(v - v_{i-\frac{1}{2}})(v - v_{i+\frac{1}{2}})$ multiplied by two different constants

$$Q[v_{i-\frac{3}{2}}, v_{i-\frac{1}{2}}, v_{i+\frac{1}{2}}],\ \ and\ \ Q[v_{i-\frac{1}{2}}, v_{i+\frac{1}{2}}, v_{i+\frac{3}{2}}]. \tag{12}$$

These two constants are the two second degree divided differences of $Q(v)$ in two different stencils. We have already noticed before, in (9), that a smaller divided difference implies the function is "smoother" in that stencil. We thus decide upon which point to add to the stencil, by comparing the two relevant divided differences (12), and picking the one with a smaller absolute value, i.e. check if

$$|Q[v_{i-\frac{3}{2}}, v_{i-\frac{1}{2}}, v_{i+\frac{1}{2}}]| < |Q[v_{i-\frac{1}{2}}, v_{i+\frac{1}{2}}, v_{i+\frac{3}{2}}]|. \tag{13}$$

This step can be continued, with one point added to the stencil at each step, according to the smaller of the absolute values of the two relevant divided differences, until the desired number in points in the stencil is reached. In general, to get a $m-th$ order interpolating polynomial, we need a stencil with $m+1$ points.

For the same piecewise quadratic interpolation to the piecewise linear function, but this time using the ENO procedure, we obtain a non-oscillatory interpolation. ENO reconstruction is uniformly high order accurate right up to the sharp-transition region. It achieves the effect by adaptively choosing the stencil based on the absolute values of divided differences. In practice, the stencil might change even by a round-off error perturbation near zeroes of the derivatives of the solution. A "biasing" strategy can be used to remedy this problem.

One also needs to consider the smoothness in multi-dimensions. Even though the curves are monotone along grid lines in all directions, the interpolated values in the interpolating cube can still be oscillating. This can happen because of the non-smooth change in the curvature of the interpolating polynomials. Hence we extend the ENO idea into multi-dimensions. When we determine the interpolating polynomial along grid lines, we not only use the dynamic stencil along that grid line to achieve 1-d smoothness, but also check the neighboring function values in other directions to ensure a smooth change of the curvature of the interpolating polynomials in all directions.

3. TRANSFINITE BLENDING FUNCTIONS

Device models usually are described with charge and current functions with three voltages as independent variables. To best reflect the original model, multidimensional tables needs to be used. The interpolation along one-dimensional grid lines is reconstructed to the three-dimensional space. Our reconstruction is cell-based. Interpolation values on the edges are blended with the values on the grid points to reconstruct function values in multidimensional voltage space.

In obtaining approximate device evaluation for device model q, i, g, and c in the general m-dimensional voltage space, $\Omega \subset \mathsf{V}^m$, enclosed by the boundary $\delta\Omega$, we employ polynomial approximations. The most natural and computationally efficient extension to several dimensions appears through the use of tensor products. We construct Ω using K non-overlapping general hexahedrals, $\mathsf{D}^k \subset \mathsf{V}^m$, such that

$$\Omega = \bigcup_{k=1}^{K} \mathsf{D}^k \ , \ \delta\Omega = \bigcup_{k=1}^{K} \delta\mathsf{D}_{kk} \ , \ \delta\mathsf{D}^k = \bigcup_{i=1}^{K} \delta\mathsf{D}_{ki} \ ,$$

where $\delta\mathsf{D}_{kk} = \mathsf{D}^k \cap \delta\Omega$ and $\delta\mathsf{D}_{ki} = \mathsf{D}^k \cap \mathsf{D}^i$ for $i \neq k$, and there exists a diffeomorphism, $\Psi : \mathsf{D}^k \to \mathsf{I}$, where $\mathsf{I} \subset \mathsf{V}^m$ is the unit cube, i.e. $\mathsf{I} \in [-1,1]^m$. For efficiency of the table model evaluation, the non-overlapping D^k we use is usually rectangular in shape.

For simplicity, we shall denote D^k by D with boundary $\delta\mathsf{D}$, refer to any rectangular table cell, and we term the coordinates, $x \in \mathsf{D}$, as (v_1, v_2, v_3) or (ξ, η, ζ), interchangeably. We define $\Xi_L = \Xi_L^\xi \times \Xi_L^\eta \times \Xi_L^\zeta$, through the subsets

$$\Xi_L^\xi = \{\bar{i} | \bar{i} \in [0, \ldots, L_\xi]\} \ , \ \Xi_L^\eta = \cdots \ , \ \Xi_L^\zeta = \cdots \ .$$

Associated with these sets are the nodal sets

$$\Lambda_L^\xi(\Xi_L^\xi) = \{\xi_{\bar{i}}\}_{\bar{i}=0}^{L_\xi} \ , \ \Lambda_L^\eta(\Xi_L^\eta) = \{\eta_{\bar{j}}\}_{\bar{j}=0}^{L_\eta} \ , \ \Lambda_L^\zeta(\Xi_L^\zeta) = \{\zeta_{\bar{k}}\}_{\bar{k}=0}^{L_\zeta} \ ,$$

with the global nodal set, $\Lambda_L(\Xi_L) = \Lambda_L = \Lambda_L^\xi \times \Lambda_L^\eta \times \Lambda_L^\zeta$. The nodal sets are assumed to be ordered such that $\xi_0 = \eta_0 = \zeta_0 = -1$ and $\xi_{L_\xi} = \eta_{L_\eta} = \zeta_{L_\zeta} = 1$. Likewise, for the construction of the polynomial approximation inside the domain, I, we introduce the global set $\Xi_N = \Xi_N^\xi \times \Xi_N^\eta \times \Xi_N^\zeta$, where

$$\Xi_N^\xi = \{i | i \in [0, \ldots, N_\xi]\} \ , \ \Xi_N^\eta = \{j | j \in [0, \ldots, N_\eta]\} \ ,$$

$$\Xi_N^\zeta = \{k | k \in [0, \ldots, N_\zeta]\} \ ,$$

with the corresponding nodal sets

$$\Lambda_N^\xi(\Xi_N^\xi) = \{\xi_i\}_{i=0}^{N_\xi} \ , \ \Lambda_N^\eta(\Xi_N^\eta) = \{\eta_j\}_{j=0}^{N_\eta} \ , \ \Lambda_N^\zeta(\Xi_N^\zeta) = \{\zeta_k\}_{k=0}^{N_\zeta} \ .$$

For simplicity, we shall use the notation $\Xi_N^{\xi\eta} = \Xi_N^\xi \times \Xi_N^\eta$ and likewise for various combinations of the sets. For ease of exposure, let us also introduce the global interior set, $\tilde{\Xi}_N = \tilde{\Xi}_N^\xi \times \tilde{\Xi}_N^\eta \times \tilde{\Xi}_N^\zeta \subset \Xi_N$, where

$$\tilde{\Xi}_N^\xi = \Xi_N^\xi \setminus \{0, N_\xi\} \ , \ \tilde{\Xi}_N^\eta = \Xi_N^\eta \setminus \{0, N_\eta\} \ , \tilde{\Xi}_N^\zeta = \Xi_N^\zeta \setminus \{0, N_\zeta\} \ ,$$

with the associated interior nodal set, $\tilde{\Lambda}_N$.

We will construct the global map, $\Psi : \mathsf{D} \to \mathsf{I}$, using transfinite blending functions [5].The correspondence between the two domains, expressed through the map $x = \Psi^{-1}(\xi)$, is derived from the Boolean sum

$$\begin{aligned} q = \quad & P_\xi(q) + P_\eta(q) + P_\zeta(q) \\ & - P_\xi P_\eta(q) - P_\xi P_\zeta(q) - P_\eta P_\zeta(q) + P_\xi P_\eta P_\zeta(q) \ . \end{aligned} \tag{14}$$

where we have introduced the face projectors $P_\xi(q) = \sum_{\Xi_L^\xi} N_{\bar{i}}^\xi(\xi) x(\xi_{\bar{i}}, \eta, \zeta)$, and likewise for $P_\eta(q)$ and $P_\zeta(q)$. The shape functions, $N_{\bar{i}}^\xi, N_{\bar{j}}^\eta$ and $N_{\bar{k}}^\zeta$, are nothing more than the interpolating ENO polynomials based on Λ_L^ξ, Λ_L^η and Λ_L^ζ, respectively. Using the properties of the projectors, the edge projectors become

$$P_\xi P_\eta(q) = \sum_{\Xi_L^{\xi\eta}} N_{\bar{i}}^\xi(\xi) N_{\bar{j}}^\eta(\eta) q(\xi_{\bar{i}}, \eta_{\bar{j}}, \zeta) \ ,$$

and likewise for $P_\xi P_\zeta(q)$ and $P_\eta P_\zeta(q)$, whereas the vertex projector becomes

$$P_\xi P_\eta P_\zeta(q) = \sum_{\Xi_L} N_{\bar{i}}^\xi(\xi) N_{\bar{j}}^\eta(\eta) N_{\bar{k}}^\zeta(\zeta) q(\xi_{\bar{i}}, \eta_{\bar{j}}, \zeta_{\bar{k}}) \ .$$

To simplify things further we may also apply the transfinite blending function to construct the face projectors as

$$\begin{aligned} q(\xi_{\bar{i}}, \eta, \zeta) = \quad & (P_\eta \oplus P_\zeta)(q(\xi_{\bar{i}}, \eta, \zeta)) \\ = \quad & P_\eta(q(\xi_{\bar{i}}, \eta, \zeta)) + P_\zeta(q(\xi_{\bar{i}}, \eta, \zeta)) - P_\eta P_\zeta(q(\xi_{\bar{i}}, \eta, \zeta)) \end{aligned}$$

and similarly for the remaining faces. With this reconstruction procedure, we guarantee that Q and I are continuous over all the interfaces. This is because they are constructed uniquely from the node sets on that plane, i.e. the nodes on that face and some neighboring points on that plane.

Within this formulation, the construction of the global map, or rather its inverse, becomes feasible. In what remains we assume that the shape functions are linear, i.e. $L_\xi = L_\eta = L_\zeta = 1$ and $\Lambda_L^\xi = \Lambda_L^\eta = \Lambda_L^\zeta = \{-1, 1\}$, as $N_0^\xi = (1-\xi)/2$ and $N_1^\xi = (1+\xi)/2$ and is similar fashion for N_j^η and N_k^ζ. Thus, to construct the map we need to specify a parametric form for the edges enclosing D, e.g. $q(\xi, -1, -1) = \sum_{\Xi_N^\xi} q(\xi_i, -1, -1) L_i^\alpha(\xi)$, where $L_i^\alpha(\xi)$ signifies the ENO approximating polynomial based on the nodal set, Λ_N^ξ, employed in I. For a thorough discussion, we can refer to [5].

4. LOCAL GRID REFINEMENT

The table model is constructed dynamically during circuit simulation. When we need to do model evaluation at an operating point, we construct the building block of the table model that contains the operating point. We construct only the building blocks that are really needed in simulation. This leads to big savings in memory and is a big advantage when one wants to apply the table model in Monte Carlo simulation or any other simulation that varies model parameter.

Because of the exponential decay or increase in device behavior, it requires very small voltage step to resolve the $i-v$ and $q-v$ curves in these regions. If one uses equally-spaced table, the size of the table can be too big and consume too much memory. One approach to solve the problem is to use non-uniform voltage steps. The ENO method works well with non-uniform grid.

The non-uniform table model is constructed efficiently during circuit simulation. If there is some sharp-transition in model evaluation output, the table needs to be refined in that region only. Our table model technology makes it possible to combine ENO approximation of different orders on different edges. For example, one may apply cubic interpolation in the exponential region of BJT's while using quadratic or even linear interpolation in "nice" regions. With the transfinite blending approach, the approximation is still smooth across shared boundaries.

5. NUMERICAL EXAMPLES

We have tested the methods in the simulation of thousands of digital, analog, RF, and mixed-signal circuits. The method turns out to be very robust. The convergence property is much better than two other table model methods we have tried, namely high-order spline interpolation and 2nd-order end-point with derivative matching interpolation. While other methods have convergence problems in many tests, all our tests converge with ENO table model method.

In the first example, we show the speed-improvement and accuracy using ENO table model in the simulation of a switched-capacitor circuit. By using the table model, we achieve a speed-up of 5 times over the same simulation using analytical model, see Table 1. In Fig. (1), it is also shown that the output voltage waveform is almost on top of that of the analytical model simulation, verifying the accuracy of our table model.

In the second example, we achieve similar accuracy of table model for the simulation of a sigma-delta converter circuit. The table model gives a speed-up of 3.5 times over analytical model, see Table 1. Table model result of the digital output waveforms after several filters, modeled by Laplace transform in simulation, is very accurate compared with analytical model result.

In the third example, a digital-analog converter is simulated. The output results of both analytical and table models agree very well with each other. In this test, we achieve a speed-up of 4.5 times with table model, see Table 1.

Figure 1: Comparison of simulation results.

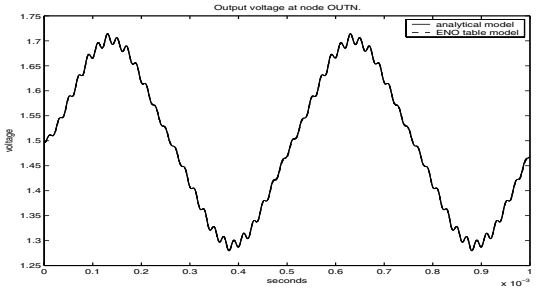

Table 1: Transient simulation time in seconds.

Model-Test	Switch-Cap Filter	Sigmadelta	D-A Converter
tabel model	1580	8900	7150
analytical model	8072	33000	32100

The final example is a full-chip RF transceiver of real design with more than 20 thousands elements. We successfully simulated the circuit with our table model while other tools failed. Even analytical model has convergence difficulty sometimes and is too slow to wait for finish. This shows ENO table model's efficiency and robustness.

6. CONCLUDING REMARKS

High-order accurate essentially non-oscillatory interpolation method is used with transfinite blending technique to construct robust, efficient, and accurate table models in circuit simulation. ENO's flexibility makes it possible to consider smoothness in multi-dimensions and do local grid refinement adaptively only in the region that need more accuracy. Need-based and on-the-fly table building during simulation greatly reduces memory consumption of the table which is important for applications such as Monte Carlo simulation. The table model technology has been proved to be robust and accurate in simulation of all types of circuits. It is becoming the first one successfully applied in prime-time Spice simulator, due to its high accuracy, besides Fast-Spice simulator. It typically improves transient analysis speed by 3 to 5 times over analytical model.

7. REFERENCES

[1] W. M. Coughran, E. Grosse, and D. J. Rose, "Variation Diminishing Splines in Simulation," *SIAM J. Sci. Stat. Comput.*, vol. 7 (1986), pp. 696-705.

[2] Peter B. L. Meijer, "Fast and Smooth Highly Nonlinear Multidimensional Table Models for Device Modeling," *IEEE Transactions on Circuits and Systems*, Vol. 37, No. 3 (1990), pp. 335-346.

[3] Chandramouli Visweswariah and Ronald A. Rohrer, "Piecewise Approximate Circuit Simulation," *IEEE Transactions on Computer-Aided Design*, Vol. 10, No, 3 (1991), pp. 861-870.

[4] A. Harten, B. Engquist, S. Osher and S. Chakravarthy, "Some results on uniformly high order accurate essentially non-oscillatory schemes," *Applied Numerical Mathematics*, v2 (1986), pp.347-377.

[5] W. J. Gorgon and C. A. Hall, Transfinite element methods: Blending-Function interpolation over arbitrary curved element domains, *Numer. Math.*, vol. 21, pp. 109-129, 1973.